

## Phase Diagrams of Ising Models on Husimi Trees II. Pair and Multisite Interaction Systems

James L. Monroe<sup>1</sup>

*Received September 24, 1992; final February 11, 1992*

---

We continue an earlier study of multisite interaction Ising spin models on Husimi trees. In particular, attention is given to systems with both a nearest-neighbor pair interaction and three-site interactions. We use our calculations of the phase diagrams of the systems on Husimi trees as approximations of systems with the same interactions but on a regular lattice, e.g., the triangle lattice. Specific models where exact results are available are used as test cases. All of the work involves computation of quantities, such as the magnetization, by iterative processes. Hence we are dealing with a discrete map and for certain values of the interaction strengths we obtain for the magnetization diagram results involving period doubling, chaos, period-three windows, etc., all phenomena of recent interest in connection with dynamical systems and now associated with certain Ising spin systems.

---

**KEY WORDS:** Ising spin; Baxter–Wu model; Husimi trees; dynamical systems; multisite interactions.

### 1. INTRODUCTION

In an earlier paper<sup>(1)</sup> (hereafter referred to as I) we showed how the calculation of the magnetization of multisite interaction (hereafter MSI) Ising spin models on Husimi trees gives rise to iterative equations. These models, where the thermal average of the spin on the central site can be calculated exactly by the use of iterative equations, were shown to be of interest both because one is able to investigate a variety of recently studied phenomena such as the effect of frustration and these systems give good approximations to the phase diagrams of Ising model systems with MSIs on more realistic lattices such as the square and triangular lattice. The

---

<sup>1</sup> Department of Physics, Beaver Campus, Penn State University, Monaca, Pennsylvania 15061.

approximations of these phase diagrams are particularly good when compared with the mean-field approximations, which have been shown to have difficulty approximating MSI systems.

In I the models presented were denoted as pure MSI systems because pair interactions were not present. However, many Ising spin systems used as models for various physical phenomena, such as the model for amphiphiles proposed by Widom<sup>(2)</sup> and the model for lipid bilayers proposed by Scott,<sup>(3)</sup> have both pair and MSIs. For this reason we present here some results on what will be called mixed interaction systems. In particular we will look at systems with two and three site interactions plus the external magnetic field.

In this paper we investigate three mixed interaction systems. In Section 2 we present the first system, a Husimi tree system used to approximate an Ising model on a Kagomé lattice with pair and three-site interactions. For this case there are exact results by Wu and Wu<sup>(4)</sup> which are used as a test to gauge the accuracy of the approximation. Next, in Section 3, we return to the system presented in I whose central site magnetization exhibited the full bifurcation cascade, chaos, etc., but we now include pair interactions and investigate their effect. In Section 4 we again investigate a system where some exact results are available for the case where only a three-site interaction is present, the Baxter–Wu model,<sup>(5)</sup> and where there has been a variety of approximation methods employed to obtain the phase diagram when pair interactions are also present.<sup>(6–10)</sup> As we will see, the comparison of our approximation of this model with previous approximations will point out the importance of the choice of an appropriate basic building block of the Husimi tree used to approximate the system as well as the impact of boundary conditions even when looking at a site deep within the tree.

## 2. ISING SPIN SYSTEM ON KAGOMÉ LATTICE

Very recently Wu and Wu<sup>(4)</sup> obtained some exact results for a mixed interaction system. In particular they considered an Ising spin system on a Kagomé lattice with Hamiltonian

$$\mathcal{H} = -J_3 \sum_{\Delta} \sigma_i \sigma_j \sigma_k - J_2 \sum_{\text{n.n.}} \sigma_i \sigma_j - h \sum_i \sigma_i \quad (1)$$

where the first sum is over all triangular faces of the lattice, the second sum is over all nearest-neighbor pairs, and the third sum is over all sites. This model they related to an eight-vertex model on the hexagonal lattice and this they showed is equivalent to an Ising model in an external field and

having nearest-neighbor interactions again on the hexagonal lattice. Since exact results are known for this last system, exact results are obtained for the original model.

One general approach to constructing an Ising spin model on a Husimi tree where two- and three-site interactions are present is to take as our basic building block a triangle consisting of three Ising spins one on each corner of the triangle. The zeroth-generation system consists of just this basic building block. For the first-generation system we attach  $\gamma - 1$  triangles at each of the two upper sites of a new base triangle (see Fig. 1a, where  $\gamma = 3$ ). Then, continuing this process, we take  $\gamma - 1$  first-generation branches and attach them to each of the upper sites of a new triangle, given us a second-generation branch (see Fig. 1b). We continue in this manner until the final step, where we take  $\gamma$ ,  $(n - 1)$ th-generation branches and attach them to each other at their base site. We denote the spin at this site as  $\sigma_0$ . In this way each site, except those on the boundary, are directly involved in the same number of interactions, e.g., for the pair interactions

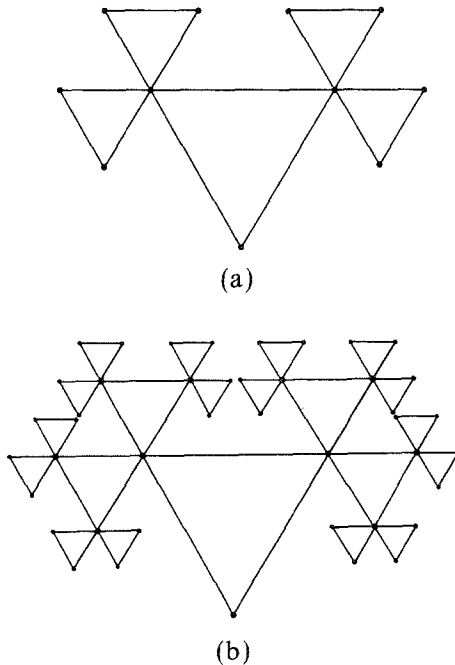


Fig. 1. (a) The first-generation branch of a Husimi tree system used to approximate the system of Wu and Wu.<sup>(4)</sup> (b) A second-generation branch for the same system. The change in the size of the triangle for various layers is done only for simplicity in illustration and represents no change in interaction strengths.

present each site has the same coordination number. Following the method of I, we can calculate the thermal average of the base site  $\langle \sigma_0 \rangle$  as

$$\langle \sigma_0 \rangle = \frac{a(z_n)^\gamma - 1}{a(z_n)^\gamma + 1} \tag{2}$$

where

$$z_n = \frac{a^2 b^2 c (z_{n-1})^{2(\gamma-1)} + 2a(z_{n-1})^{\gamma-1} + c}{a^2 (z_{n-1})^{2(\gamma-1)} + 2ac(z_{n-1})^{\gamma-1} + b^2} \tag{3}$$

and where  $a = e^{2\beta h}$ ,  $b = e^{2\beta J_2}$ ,  $c = e^{2\beta J_3}$ , and  $\beta = 1/kT$ . Equations (2) and (3) are counterparts of Eqs. (7) and (8) of I. As in I, the phase diagram is determined by the properties of the rational map given by (3).

Now for an approximation of the Kagomé lattice we want to let  $\gamma = 2$ . Wu and Wu found the critical surface in the  $u, v$ , and  $w$  space, where they defined  $u = e^{-\beta h}$ ,  $v = e^{-4\beta J_2}$ , and  $w = e^{-2\beta J_3}$ . For ease of comparison we take three slices through this space, one at  $v = 0.05$ , another at  $v = 0.10$ , and finally one at  $v = 0.15$ . Also, there is a symmetry present in this model, which shows we need only look at  $u \geq 1.0$  (this symmetry is present in our approximation as well). This symmetry indicates that the magnetization remains unchanged when  $h \rightarrow -h$ , i.e.,  $u \rightarrow 1/u$ , and  $J_3 \rightarrow -J_3$ , i.e.,  $w \rightarrow 1/w$ . The presence of this symmetry indicates that Eq. (7) of ref. 4 must contain an error, since as written the equation does not reflect this symmetry. The first term should be  $v^3 w^2$  rather than  $v^2 w^2$ .<sup>(11)</sup> The comparisons for the three values of  $v$  are shown in Fig. 2. In all three cases the results of the approximation closely match the exact results. Note that, as is often the case where MSIs are present, phase transitions occur at  $h \neq 0$ .

For the special case  $J_3 = 0$ , i.e.,  $c = 1$ , the map has a fixed point at  $z = 1$  when  $h = 0$ . One can see this by inspection of Eq. (3). This fixed point

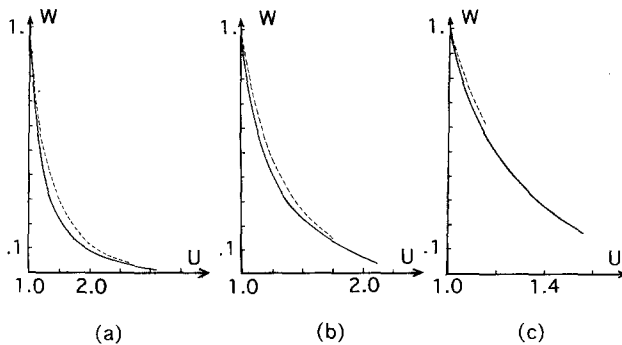


Fig. 2. Comparison of Husimi tree approximation with exact results of ref. 4. (a)  $v = 0.05$ , (b)  $v = 0.10$ , and (c)  $v = 0.15$ . The solid line (dashed line) represents the results of approximation (exact results).

for high temperature  $T$ , that is, small  $\beta J_2$ , is a stable fixed point, meaning that  $\langle \sigma_0 \rangle = 0$  at  $h=0$ . However, as we lower  $T$ , that is, raise  $\beta J_2$  and hence  $b$ , at some value the fixed point becomes unstable and it is just this value of  $\beta J_2$  which gives the critical point. This point can be found analytically and occurs at  $b = \sqrt{5}$ . For this special situation,  $J_3 = 0$ , mean-field theory gives  $\beta J_2 = 1/4$ , the standard Cayley tree approach with coordination number equal to 4 gives  $\beta J_2 = 0.3466$ , and our Husimi tree approach gives  $\beta J_2 = (1/4) \ln(5) = 0.4024$ . The exact result is  $\beta J_2 = (1/4) \ln(3 + 22 \cdot 3) = 0.4666$ . Therefore, compared to other closed-form approximations of  $\beta J_2$ , the results are an improvement. It should also be mentioned that Wu and Wu conjecture that phase transitions occur in no other regions of the  $u-v-w$  space. Our numerical computations support this conjecture.

It is of some interest to examine the mathematical mechanisms which cause a jump in the value of the fixed point and therefore result in a discontinuity of  $\langle \sigma_0 \rangle$ . In I we found a first-order phase transition for a system of the variety just described with the specific values of  $\gamma = 3$ ,  $J_2 = 0$ , and  $J_3 > 0$ . Here the discontinuity in the value of the fixed point and hence the discontinuity of the order parameter was caused by one of the stable fixed points vanishing as the magnetic field  $h$  is increased (see Fig. 3). This

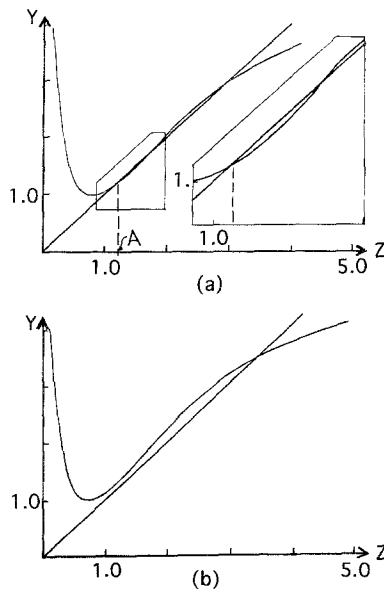


Fig. 3. (a) A plot of  $y=z$  and  $y=g(z)$  for  $\gamma=3$ ,  $J_2=0$ ,  $J_3=0.8$ , and  $h=0.22$ , with the insert being a blowup of the region around the stable fixed point  $z=A$ . (b) A similar plot, but for  $h=0.30$ .

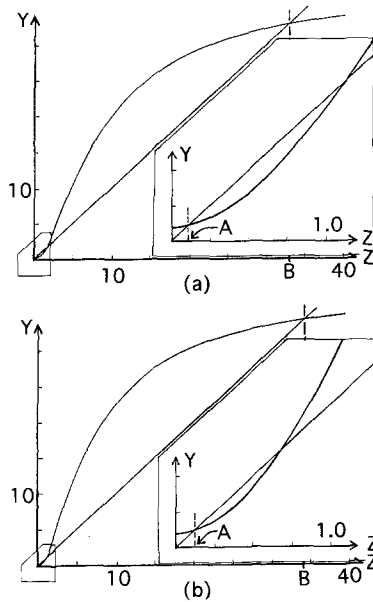


Fig. 4. A plot of  $y=z$  and  $y=g(z)$  for  $\gamma=2$ ,  $J_2=0.7489$ ,  $J_3=0.3466$ , and  $h=-0.20$ , with the insert being a blowup around the stable fixed point  $z=A$ . (b) A similar plot, but for  $h=-0.10$  again with insert.

is to be contrasted with the case studied here with  $\gamma=2$ ,  $J_2>0$ , and no restriction on  $J_3$ . In this case, as shown in Fig. 4, the boundary between the basins of attraction of fixed points  $A$  and  $B$  moves from  $z>1$  at  $h=-0.2$  to  $z<1$  at  $h=-0.1$ . Since with free boundary conditions one starts the iterations of Eq. (3) with  $z=1$ , as  $h$  is varied one moves from one basin of attraction to the other, causing a discontinuity of the order parameter. Hence we have two very different mathematical mechanisms causing first-order phase transitions.

### 3. ISING SPIN SYSTEM ON TRIANGLE LATTICE WITH $\gamma=3$

If one lets  $\gamma=3$  in Eqs. (2) and (3) rather than  $\gamma=2$ , the plots of  $\langle\sigma_0\rangle$  vs.  $h$  and hence the phase diagram change dramatically. The  $\gamma=3$  case can be used to approximate a triangle lattice with  $J_3$  interactions on all down-pointing or up-pointing triangles but not both. As we showed in I for the case where there was no pair interactions, if  $J_3<0$ , one obtains plots of  $\langle\sigma_0\rangle$  vs.  $h$  showing full "period-bubbling" bifurcations, chaos, period-three windows, etc. The reason for this is that we have the presence of frustration effects. If we set  $J_3=-1$  and vary the temperature as we did in I, then for

large  $T$  one gets no phase transitions and  $\langle \sigma_0 \rangle$  is simply a monotonically increasing function of  $h$  for  $h > 0$ . If we lower  $T$ , at some point we find that there is a single bubble in the plot of  $\langle \sigma_0 \rangle$  vs.  $h$ . Hence, rather than period-doubling, we have what has been denoted by Bier and Bountis<sup>(10)</sup> as “period-bubbling.” Physically, for small  $h$  the interaction  $J_3$  dominates, while for large  $h$ ,  $h$  dominates. In the intermediate region we have the bubble (see I). As we continue to lower  $T$ , new bubbles form as part of the old bubbles, and for still lower  $T$ 's we reach a region where for intermediate values of  $h$  we have chaos.

The question we want to address in this section is, what effect does the introduction of n.n. pair interactions  $J_2$  have on the plots of  $\langle \sigma_0 \rangle$  vs.  $h$ ? The plots themselves are the best indicators of this and we show in Fig. 5–8 a series of such plots. Specifically, we use Figs. 6b and 7a as our reference point, since in these cases  $J_2 = 0$ . In this case  $J_3 = -1$  and we set  $T = 0.3$ , which is low enough to cause the plot of  $\langle \sigma_0 \rangle$  vs.  $h$  to show a full period-bubbling cascade, with regions of the  $h$  axis where one has chaos, period-three windows, etc. In our sequence of figures we let the value of  $J_2$  vary from 0.3 (Fig. 5a) to  $-1.0$  (Fig. 8c). For the extreme values  $J_2 = 0.3$  and  $J_2 = -1.0$  the pair interaction, due to its strength, has eliminated the frustration effects. As Fig. 5a shows, with  $J_2 = 0.30$  we have a single first-order phase transition. However, the transition does not occur at  $h = 0$  as it must for  $J_2 > 0$  and  $J_3 = 0$ . The effect of  $J_3$  is to shift the phase transition to a point where  $h > 0$ . Now as  $J_2$  is lowered in value toward  $J_2 = 0$  the frustration effects increase. However, while the period bubbling begins to appear, it is now what might be categorized as “chopped period-bubbling,”

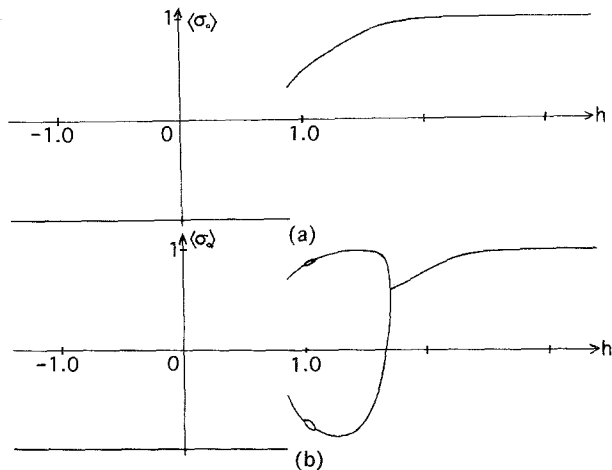


Fig. 5. Plot of  $\langle \sigma_0 \rangle$  versus  $h$  for  $\gamma = 3$ ,  $J_3 = -1.0$ ,  $T = 0.30$ , and (a)  $J_2 = 0.30$ , (b)  $J_2 = 0.20$ .

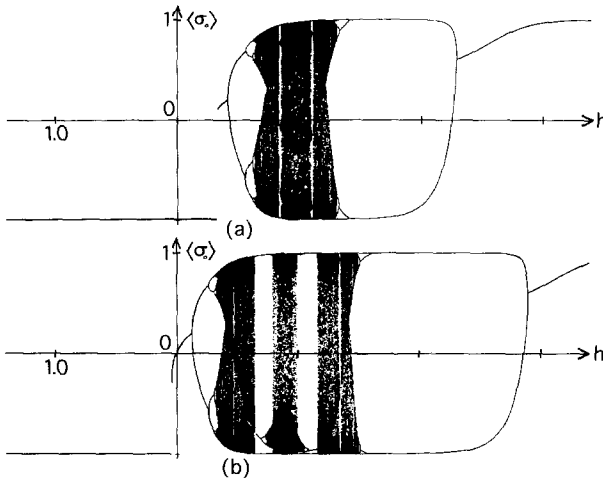


Fig. 6. Plot of  $\langle \sigma_0 \rangle$  versus  $h$  for  $\gamma = 3$ ,  $J_3 = -1.0$ ,  $T = 0.30$ , and (a)  $J_2 = 0.10$ , (b)  $J_2 = 0.0$ .

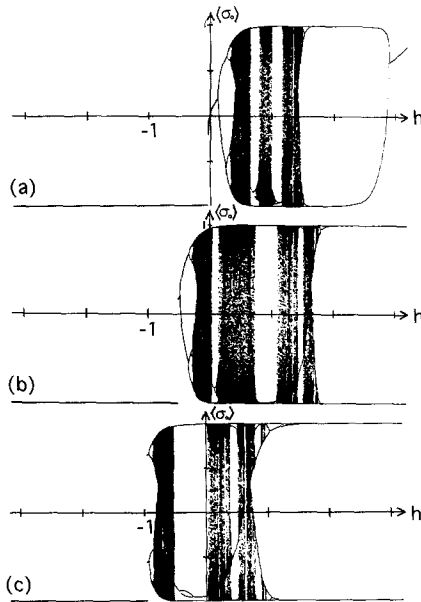


Fig. 7. Plot of  $\langle \sigma_0 \rangle$  versus  $h$  for  $\gamma = 3.0$ ,  $J_3 = -1.0$ ,  $T = 0.30$ , and (a)  $J_2 = 0.0$ , (b)  $J_2 = -0.20$ , (c)  $J_2 = -0.040$ .



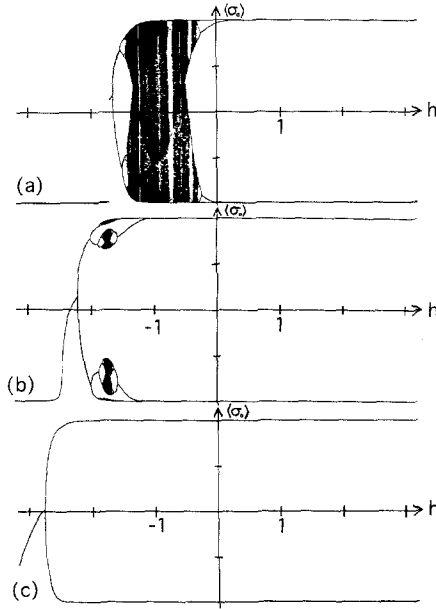


Fig. 8. Plot of  $\langle \sigma_0 \rangle$  versus  $h$  for  $\gamma=3.0$ ,  $J_3 = -1.0$ ,  $T=0.30$ , and (a)  $J_2 = -0.60$ , (b)  $J_2 = -0.80$ , (c)  $J_2 = -1.00$ .

as best illustrated in Fig. 5b, where the left segment of the large bubble is missing.

In Fig. 7a we again show the case where  $J_2 = 0$ . Then in Figs. 7b and 7c and Figs. 8a–8c we lower  $J_2$  from  $-0.2$  to  $-1.0$ . Here again as we make  $J_2$  more antiferromagnetic the pair interaction lessens the frustration effect of  $J_3$ . With  $J_2 = -1.0$  we have reached a point where we move from a region for large negative  $h$  field, where we have a fixed point, to, for  $h$  closer to zero, a stable 2-cycle as found by Thompson<sup>(12)</sup> for the antiferromagnetic n.n. pair interaction system on the standard Cayley tree.

#### 4. THE BAXTER–WU MODEL AND ITS GENERALIZATIONS

Another of the very small number of lattice spin systems with MSIs where exact results have been obtained is known as the Baxter–Wu model. It consists of a triangular lattice with three-site interactions on all elementary triangles of the lattice. As shown by Baxter and Wu,<sup>(5)</sup> there is a phase transition at  $h=0$  and the critical point is given by  $\sinh(2\beta J_3) = 1$ . This is to be contrasted with an MSI system discussed in I which consisted of a lattice spin system again on a triangular lattice with three-site interac-

tions only on all down-pointing *or* up-pointing basic triangles of the lattice but not both. Then one has a phase transition generally at  $h \neq 0$  and only for  $T=0$  does the phase transition occur at  $h=0$ . Hence there is a sharp contrast between the two systems. This contrast will manifest itself in the need to choose a different basic building block for approximation of the Baxter–Wu model.

It may seem natural to approximate the Baxter–Wu model with the same Husimi tree system as used in I and Section 3, with a single triangle consisting of three sites as the basic building block, but now with  $J_2=0$  and  $\gamma=6$ . However, this is not an appropriate choice. This system produces a phase diagram similar to that found with  $J_2=0$  and  $\gamma=3$  as presented in I, where it was used to approximate the system of the preceding paragraph. This reflects the fact that these Husimi tree systems approximate regular lattice systems which have only a one-element translationally-invariant family of bonds in the sense of Slawny.<sup>(13)</sup>

To reflect the fact that in the Baxter–Wu model we have three-site interactions on both up-pointing *and* down-pointing triangles, we can select a basic building block which consists of a diamond-shaped system made up of two triangles (see Fig. 9a). Using this as our basic building block and again denoting the basic building block as the zeroth-generation system, we construct a first-generation system by attaching  $\gamma - 1$  basic building blocks only at the upper site of the new diamond-shaped base building block, (see Fig. 9b, where  $\gamma = 3$ ). We continue in this manner until the final step, where we take one  $(n + 1)$ th-generation system and to its bottom site we attach  $(\gamma - 1)$ ,  $n$ th-generation systems (see Fig. 9c). In this manner the top and bottom sites of the basic building blocks now have  $\gamma$  blocks attached,

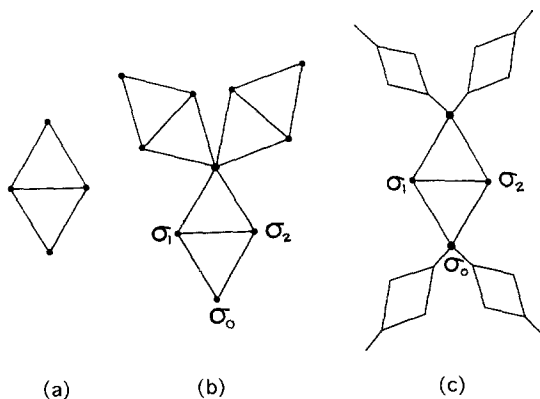


Fig. 9. (a) The zeroth-generation diamond-shaped building block. (b) A first-generation system. (c) The final symmetric system. The symbol  $\diamond$  represent  $n$ th-generation branches.

except of course for those basic building blocks on the boundary of the tree.

One can again rather easily obtain equations similar to Eqs. (2) and (3) for the previous system, which allows one to calculate  $\langle \sigma_0 \rangle$ . For approximating the triangle lattice one takes  $\gamma = 6$ . Doing so, one finds a line of phase transitions at  $h = 0$  with a critical point given by  $\beta J_3 = 0.4812$ . The results of Baxter and Wu show  $\beta J_3 = 0.4407$ . Thus, one sees that for the Baxter–Wu model at  $h = 0$ , the change of basic building blocks results in a qualitatively correct phase diagram and one quantitatively within 10% of the exact result.

As mentioned earlier, there are a number of approximations of the Baxter–Wu model for  $h \neq 0$  as well as  $h = 0$ . The model has been studied by mean-field theory,<sup>(6)</sup> the interface method,<sup>(7)</sup> the renormalization group approach,<sup>(8)</sup> the variational method of Baxter,<sup>(9)</sup> and by Monte Carlo techniques.<sup>(10)</sup> At  $T = 0$  analysis indicates a transition at  $h = -6J_3$  between a state with all spins pointing down to one with a down spin on two lattice sites of each elementary triangle and the remaining site having an up spin. Hereafter this will be denoted as  $(+ - -)$ . Therefore, rather than looking at  $\langle \sigma_0 \rangle$ , it is appropriate to look at  $\langle \sigma_0 + \sigma_1 + \sigma_2 \rangle = 3m$ , where 0, 1, and 2 are the three sites of a triangle as in Fig. 9b or 9c. For  $T = 0$ , then, one has for  $h < -6J_3$  that  $m = -1$ , while for  $-6J_3 < h < 0$  one has  $m = -1/3$ , and finally for  $h > 0$ ,  $m = 1$ . For small  $T$ , in particular  $T = 0.05$  and  $J_3 = 1$ , our Husimi tree approximation results in  $m$  as shown in Fig. 10a. We see the first-order transition mentioned above at  $h = 0$ . Also, one can see an abrupt change in the value of  $m$  from  $-1$  to  $-1/3$  in the vicinity of  $h = -6$ . However, there is no true phase transition, either a first- or second-order transition at  $k \neq 0$ . Hence the model is not sensitive enough to replicate the phase transition at  $h \neq 0$ , which is supposed to be a second-order transition.

The emphasis of the preceding sections of this paper has been on mixed interaction systems, i.e., those with both pair interactions and MSIs. One can easily generalize the Baxter–Wu model by adding a nearest neighbor pair interaction  $J_2$ . References 6–10 have looked at this generalized system and have found approximate phase diagrams as the strength of  $J_2$  is varied. If we define  $r = J_3/J_2$  and we take  $J_3 > 0$  and  $J_2 > 0$ , then at  $T = 0$  for  $r > 3/2$  we have three phases. For large, positive  $h$  we have all spins up, for large, negative  $h$  we have all spins down, and for intermediate  $h$  we have the  $(+ - -)$  configuration. For  $0 < r < 3/2$  the ground state undergoes only the transition from all spins up to all spins down as  $h$  is lowered in value. The  $T = 0$  analysis in ref. 9 gives as a function of  $r$  the locations on the  $h$  axis where the transitions are to take place.

To approximate the generalized Baxter–Wu model, our diamond-

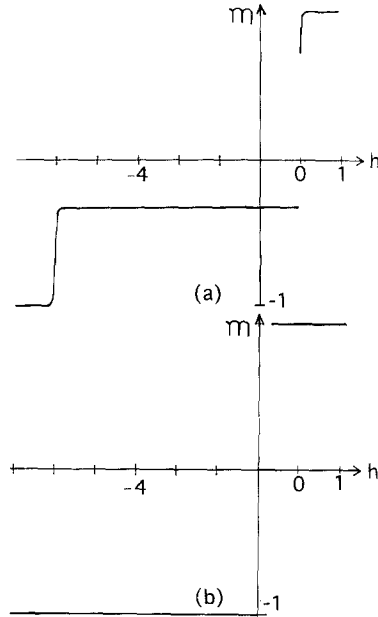


Fig. 10. The three-site magnetization  $m$  versus  $h$  for the diamond-shaped building block system. (a)  $\gamma = 6$ ,  $T = 0.05$ ,  $J_3 = 1.0$ , and  $J_2 = 0.0$ . (b)  $\gamma = 6$ ,  $T = 0.05$ ,  $J_3 = 1.0$ , and  $J_2 = 1.0$ .

shaped basic building block has added to it n.n. pair interactions of strength  $J_2$ . For  $r = 1$  and  $T = 0.05$  the model gives a transition from the basically spin-down configuration to the spin-up configuration, as it should for low  $T$  (see Fig. 10b). However, the transition occurs at approximately  $h = -0.67$ , while it should occur at approximately  $h = -2.0$ . At  $T = 0$  the transition should occur at exactly  $h = -2$ , yet for our present treatment a  $T = 0$  analysis shows that the transition occurs at  $h = -2/3$ .

At this point we need to consider in more detail various aspects of how we arrive at the recursion relation, the equation similar in nature to Eq. (3), but for the diamond-shaped building block case, where now we need not only  $\langle \sigma_0 \rangle$ , but also  $\langle \sigma_1 \rangle$  and  $\langle \sigma_2 \rangle$ . As previously stated, all top and bottom sites of the diamond-shaped building blocks have  $\gamma$  triangles attached to them except those on the boundary. Since we want to be able to calculate  $\langle \sigma_0 \rangle$ , the thermal average of the base site of the central diamond and  $\langle \sigma_1 \rangle$  or  $\langle \sigma_2 \rangle$ , the thermal average of the side sites of the central diamond,  $\langle \sigma_1 \rangle = \langle \sigma_2 \rangle$  by symmetry, we must keep track of four terms. We denote  $A_n$  ( $D_n$ ) to account for the  $n$ th-generation branch with

both spins + (−) and  $B_n$  ( $C_n$ ) to account for the  $n$ th-generation branch with the bottom site + (−) and the side site − (+). We have

$$A_n = a^3 b^4 c^2 z_{n-1}^{\gamma-1} + a^2 b z_{n-1}^{\gamma-1} + a^2 b^2 c + abc \tag{4a}$$

$$B_n = a^2 b z_{n-1}^{\gamma-1} + a c^2 z_{n-1}^{\gamma-1} + abc + b^2 c \tag{4b}$$

$$C_n = a^3 b^2 c z_{n-1}^{\gamma-1} + a^2 b c z_{n-1}^{\gamma-1} + a^2 + abc \tag{4c}$$

$$D_n = a^2 b c z_{n-1}^{\gamma-1} + a b^2 c z_{n-1}^{\gamma-1} + abc^2 + b^4 \tag{4d}$$

where

$$z_{n-1} = \frac{A_{n-1} + B_{n-1}}{C_{n-1} + D_{n-1}} \tag{5}$$

and where  $a$ ,  $b$ , and  $c$  are as defined following Eq. (3). Then when completing the Husimi tree as described above we obtain

$$\langle \sigma_n \rangle_{n+1} = \frac{a(A_n + B_n)z_{n-1}^{\gamma-1} - (C_n + D_n)}{a(A_n + B_n)z_{n-1}^{\gamma-1} + (C_n + D_n)} \tag{6}$$

$$\langle \sigma_1 \rangle_{n+1} = \frac{a(A_n - B_n)z_{n-1}^{\gamma-1} + (C_n - D_n)}{a(A_n + B_n)z_{n-1}^{\gamma-1} + (C_n + D_n)} \tag{7}$$

For the above equations, each elementary triangle has a  $J_3$  interaction, each n.n. pair has a  $J_2$  interaction, and each site has a full  $h$  field present. But each site *should not* have a full  $h$  field associated with it for correct  $T=0$  behavior.

To emphasize how various  $h$ -field contributions can come about, we focus attention on what was done in the computation of Eqs. (4)–(7). Here we started with a single building block and assumed there is a full  $h$  field on each of the three upper sites to compute  $A_1$ ,  $B_1$ ,  $C_1$ , and  $D_1$ . The bottom site  $h$ -field is taken into account when we construct the second-generation branch, where again we will take account of a full  $h$  field on the three upper sites of the basic building block. The uppermost site is where the first-generation branch is attached, and therefore the  $h$ -field contribution of the bottom site of the first-generation branch is taken into account when constructing the second-generation branch. We continue in this manner until we complete the tree. At this point the missing  $h$ -field term is taken care of by the factor  $a$  found in both Eqs. (6) and (7). Thus we end with a system with a full  $h$  field on each site.

To see how one might go about the construction of a slightly different expression for the calculation of  $\langle \sigma_1 \rangle_{n+1}$  and  $\langle \sigma_0 \rangle_{n+1}$ , one could note that since each top and bottom site of a diamond (except boundary sites)

is connected to  $\gamma$  triangles, one can divide up the contribution of the  $h$  field on these sites by this factor. Hence we associate with each top or bottom site of a diamond this  $h/\gamma$ -field term. As we build up our full symmetric Husimi tree (as in Fig. 9c), each of these sites then gets eventually a full  $h$ -field term except those which are the boundary sites; these have only  $h/\gamma$ . However, as a number of authors have pointed out,<sup>(14-16)</sup> for the standard Cayley tree or Bethe lattice the number of boundary sites grows exponentially as the tree is expanded, so the boundary sites never become insignificant. The same occurs here with these Husimi tree systems.

To be consistent, the side sites must also be reconsidered. They are boundary sites as well because no attachment is made to them. However, since each side site is shared among two triangles, the  $h$ -field contribution they receive should be  $2h/\gamma$ . None of these considerations arise regarding the approximation of a pair interaction system by the standard Bethe lattice approach<sup>(17)</sup> because in this case phase transitions occur only at  $h = 0$ .

With this adjustment the Husimi tree approximation of the systems with  $r < 3/2$  is qualitatively correct and in addition reasonably good quantitatively for the first-order transitions resulting from transitions between states with predominately up spins to states with predominately down spins as is the case for  $r = 1$ . For  $T = 0$  the locations of these transitions are *exactly* where they should be. However, for the case of  $r > 3/2$  and small temperatures we have first-order transitions from the  $(+ - -)$  state to the  $(+ + +)$  state but not at the correct  $h$  value for  $T = 0$ .

Thus, by taking into account the differences between the placement of sites in our Husimi tree construction as it pertains to the  $h$ -field contributions, we have improved our approximation, but we should not stop here. The n.n. pair interactions are really of two types—type A, those on the sides of the diamond; and type B, those across the center of the diamond-shaped building blocks. At our points of contact between the building blocks we need  $\gamma = 6$  to meet the criteria of having six  $J_3$  interactions of the connecting site. But this then means there are twelve  $J_2$  interactions at a site. We should set each of these at a value of  $J_2/2$  since each n.n. pair interaction is shared between two triangles in the triangle lattice we are trying to approximate. Now the type B n.n. interactions in our Husimi tree construction are already shared by two triangles, so no adjustment in their value is need; they remain  $J_2$ .

With this final refinement for all values of  $r$  the first-order phase transitions occur for  $T = 0$  at their proper  $h$  values and for nonzero  $T$  the line of first-order phase transitions in the  $h$ - $T$  plane is in reasonable quantitative agreement and definite qualitative agreement with all other forms of approximation mentioned previously. See Fig. 11 for comparison of the

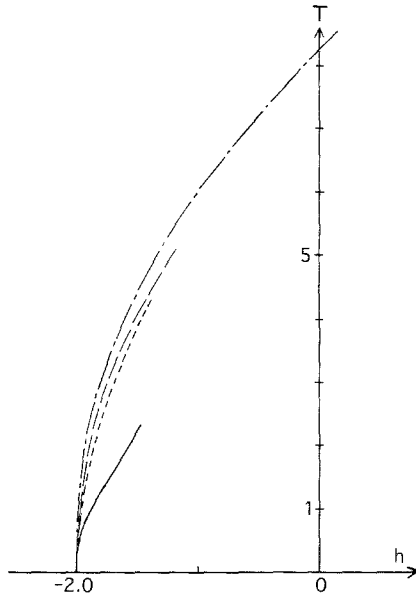


Fig. 11. Approximations of the phase diagram of the generalized Baxter-Wu model with  $r=1.0$ . The dotted line is the Monte Carlo result,<sup>(10)</sup> the dashed line the variational approximation,<sup>(9)</sup> the dot-dash line the mean-field results,<sup>(6)</sup> and the solid line the Husimi tree approximation result.

$r = 1$  case with mean-field, Monte Carlo, and variational method results. It would be a significant improvement to find a basic building block which would result in a system giving better approximation to the line of second-order phase transitions present. We have not been successful in finding such a situation. For the full range of  $r$  values the phase diagrams are quite varied and it should be pointed out that some of the other approximation schemes previously referred to have also had qualitative problems in regard to exhibiting correct phase diagrams. For example, the interface method<sup>(7)</sup> can only locate second-order phase transitions and both the mean-field<sup>(6)</sup> and variational approach<sup>(9)</sup> show phase transitions for small  $h > 0$  which, while not rigorously proven not to exist, are not seen in other approximations. Also, both these approximations have, where lines of second-order transitions are supposed to appear, first-order transitions. The jumps in magnetization for the variational approach are small in magnitude and get smaller as higher approximations are made, so that it is argued that the infinite-order case *would* yield second-order transitions.

## ACKNOWLEDGMENTS

The author would like to thank the Physics Department at Northeastern University, and especially Prof. F. Y. Wu, where some of the refinements on the generalized Baxter–Wu model took place.

## REFERENCES

1. J. L. Monroe, *J. Stat. Phys.* **65**:255 (1991).
2. B. Widom, *J. Chem. Phys.* **88**:6508 (1984).
3. H. L. Scott, *Phys. Rev. A* **37**:263 (1988).
4. X. N. Wu and F. Y. Wu, *J. Phys. A: Math. Gen.* **22**:L1031 (1989).
5. R. J. Baxter and F. Y. Wu, *Phys. Rev. Lett.* **31**:1294 (1973); *Aust. J. Phys.* **27**:357 (1974).
6. S. Froyen, Aa. S. Svdbø, and P. C. Hemmer, *Physica* **85A**:399 (1976).
7. J. Doczi-Reger and P. C. Hemmer, *Physica* **109A**:541 (1981).
8. M. Schick, J. S. Walker, and M. Wortis, *Phys. Rev. B* **16**:2205 (1977).
9. A. Malakis, *J. Stat. Phys.* **27**:1 (1982).
10. K. K. Chin and D. P. Landau, *Phys. Rev. B* **36**:275 (1987).
11. F. Y. Wu, Private communication.
12. C. J. Thompson, *J. Stat. Phys.* **27**:441 (1982).
13. J. Slawny, in *Phase Transition and Critical Phenomena*, Vol. 11, C. Domb and J. J. Lebowitz, eds. (Academic Press, 1986).
14. T. P. Eggarter, *Phys. Rev.* **89**:2989 (1974).
15. J. VonHeimburg and H. Thomas, *J. Phys. C* **7**:3433 (1974).
16. E. Muller-Hartman and J. Zittartz, *Phys. Rev. Lett.* **33**:893 (1974).
17. R. J. Baxter, *Exactly Solved Models in Statistical Mechanics* (Academic Press, 1982), Chapter 4.